European Journal of Pharmaceutics and Biopharmaceutics 144 (2019) 125–131

Contents lists available at ScienceDirect

European Journal of Pharmaceutics and Biopharmaceutics

journal homepage: www.elsevier.com/locate/ejpb

Research paper

Intestinal enzyme delivery: Chitosan/tripolyphosphate nanoparticles providing a targeted release behind the mucus gel barrier

Christina Leichner, Max Jelkmann, Felix Prüfert, Flavia Laffleur, Andreas Bernkop-Schnürch*

Center for Chemistry and Biomedicine, Department of Pharmaceutical Technology, Institute of Pharmacy, University of Innsbruck, Innrain 80/82, 6020 Innsbruck, Austria

ARTICLE INFO

Keywords:
Chitosan, tripolyphosphate
Nanoparticles
Alkaline phosphatase
Enzyme delivery
Targeted release

ABSTRACT

Aim: The aim of this study was to evaluate the potential of chitosan/tripolyphosphate (TPP) nanoparticles to provide a targeted release of β-galactosidase behind the intestinal mucus gel barrier.
Methods: Nanoparticles were prepared by ionic gelation of chitosan and TPP in the presence of β-galactosidase. Particles were characterized regarding size, polydispersity index and drug load. Target mediated hydrolysis of the TPP cross-linker followed by particle degradation and release of β-galactosidase was investigated during incubation with isolated as well as cell and tissue associated intestinal alkaline phosphatase (IAP). Phosphate content in the media was quantified *via* malachite assay, whereas particle disintegration was monitored in parallel by measuring the decrease in particle size as well as in optical density at 600 nm. The released amount of β-galactosidase was either determined utilizing bicinchoninic acid (BCA) protein detection or *via* an enzymatic activity assay with 2-nitrophenyl β-D-galactopyranoside (ONPG) as substrate. Protection towards tryptic degradation was verified by ONPG assay.
Results: The size of nanoparticles was 573 ± 34 nm and a payload of 376 ± 18 µg β-galactosidase per mg particles was achieved. Degradation studies with isolated IAP revealed a maximum phosphate cleavage of 118 ± 1 µg/mg particles, a size decrease up to 38 ± 7 % and a release of 58 ± 0.5 % β-galactosidase. Release of 94 ± 6 % of the incorporated initial amount of β-galactosidase was proven after 3 h incubation on porcine mucosa. Furthermore a protection against tryptic degradation was attained resulting in a 3-fold higher residual enzymatic activity of encapsulated β-galactosidase compared to a control of free enzyme.
Conclusion: Chitosan/TPP nanoparticles seem to be qualified as a suitable carrier for a targeted delivery of active ingredients to mucosal tissues expressing alkaline phosphatase.

1. Introduction

The development of oral delivery systems for therapeutic biomacromolecules such as enzymes, peptides or antibodies guaranteeing their stability in the intestine is still challenging. Especially in the case of enzymes, activity has to be preserved in this hostile environment but it is from a formulator's point of view difficult to avoid premature degradation by intestinal proteases. Strategies to face these issues are focusing on the co-administration of protease inhibitors, physicochemical modifications of the macromolecules or the design of nanoparticulate-based carriers to increase proteolytic stability [1,2].

In this context, chitosan nanoparticles cross-linked with tripolyphosphate (TPP) have been widely investigated for the delivery of biologics until now [3–6]. Nevertheless the applicability of this carrier system was not examined yet in respect of a targeted release at the brush border membrane in the small intestine involving alkaline phosphatase. Intestinal alkaline phosphatase (IAP) is present in the brush border membrane of the enterocyte of the small intestine and catalyzes the nonspecific hydrolysis of phosphate esters into inorganic phosphate and alcohol. Besides, polyphosphates including tripolyphosphate are prone to degradation by IAP [7–9]. As a result of this, the TPP cross-links within the particle network should be hydrolyzed if the delivery system reaches the absorption membrane, particles should lose their stability and release their active ingredient.

Particularly within the field of local enzyme substitution therapy of β-galactosidase this novel approach might be promising, because the nanoparticles could provide shelter from the metabolizing intestinal environment combined with a local release behind the mucus gel barrier directly at the target location. β-Galactosidase, better known under the name lactase, is involved in the basic process in digestion of lactose. Absence or malfunction of this enzyme causes malabsorption up to lactose intolerance. Lactase replacement is an option for therapy and a

* Corresponding author.
E-mail address: andreas.bernkop@uibk.ac.at (A. Bernkop-Schnürch).

https://doi.org/10.1016/j.ejpb.2019.09.012
Received 13 August 2019; Received in revised form 12 September 2019; Accepted 13 September 2019
Available online 14 September 2019
0939-6411/

variety of preparations is available over the counter [10,11]. Limitations of the existing therapy option are changes in taste, because it is usually consumed together with dairy goods and the susceptibility to enzymatic metabolism in the lumen of the gastro intestinal tract (GIT). Facing these issues the incorporation of β-galactosidase in chitosan/TPP nanoparticles could be a purposeful alternative to improve its delivery.

2. Materials and methods

2.1. Materials

Chitoscience Chitosan 85/10 (average molecular weight ~50 kDa) was obtained from Heppe Medical Chitosan GmbH (Halle, Germany). Pierce™ BCA Protein Assay Kit was purchased from Thermo Scientific (Vienna, Austria). Sodium tripolyphosphate, phosphatase (alkaline from bovine intestinal mucosa, lyophilized powder, ≥10 DEA units/mg solid), β-galactosidase from *Kluyveromyces lactis* (≥2600 units/g), 2-nitrophenyl β-D-galactopyranoside, phosphatase inhibitor cocktail 2 and all other substances and chemicals were supplied by Sigma-Aldrich (Vienna, Austria).

HEPES-buffered saline (HBS) of pH 6.8 (1 L contains: 5.2 g HEPES, 7.9 g NaCl, 1 g glucose, 373 mg KCl, 147 mg $CaCl_2$ dihydrate), used as suspending media in all experiments.

2.2. Methods

2.2.1. Colorimetric assays

2.2.1.1. Malachite green. Phosphate content in the samples was quantified by the malachite green assay [12]. The reagent solution was prepared by dropwise addition of 6 mL of a 8 % (m/m) ammonium molybdate solution to 10 mL of a 0.15 % (m/m) solution of malachite green dissolved in a 3.6 M H_2SO_4 under vigorous stirring. Triton X-100 dissolved in demineralized water to a final concentration of 11 % (m/m) was added as a stabilizer for the formed colored product in a volume of 400 µL. Samples were analyzed by adding 100 µL reagent to 50 µL sample solution spiked with 5 µL 3.6 M H_2SO_4 and measurement of the absorbance at λ = 630 nm (TECAN Spark®, Tecan Group Ltd., Switzerland). The amount of eliminated phosphate was calculated from a calibration curve made of KH_2PO_4 with decreasing phosphate content.

2.2.1.2. Bicinchoninic acid (BCA). The BCA assay was used following the manufacturer's instructions. Briefly, 150 µL of sample was mixed with 150 µL of the working reagent in a 96-well plate and incubated for 90 min at 37 °C. Afterwards the absorbance was detected at 562 nm by using a microplate reader (TECAN Spark®, Tecan Group Ltd., Switzerland). The amount of protein was calculated from a standard curve prepared of bovine serum albumin (BSA). BSA was utilized as it is an universally accepted reference protein for total protein quantitation in colorimetric assays.

2.2.1.3. 2-Nitrophenyl β-D-galactopyranoside (ONPG). Enzymatic activity of β-galactosidase was determined with 2-nitrophenyl β-D-galactopyranoside (ONPG) [13]. In brief, 250 µL of sample were incubated with 50 µL of ONPG (12 mM dissolved in demineralized water) for 15 min at 37 °C on a water bath (1083, GFL Gesellschaft für Labortechnik mbH, Germany). The reaction was stopped after the addition of 300 µL 1 M Na_2CO_3 and absorbance was measured at 420 nm (TECAN Spark®, Tecan Group Ltd., Switzerland). A standard curve was obtained of pure β-galactosidase in decreasing concentrations.

2.2.2. Preparation of the nanoparticles

Nanoparticles were formulated *via* the ionic gelation method at room temperature [14]. Chitosan was dissolved in a 0.05 % (m/v) acetic acid solution to a concentration of 0.25 % (m/v) and the pH was adjusted to 6 by the addition of 5 M NaOH. Following a 0.2 % (m/v) solution of tripolyphosphate (TPP) in demineralized water was dropped into the chitosan solution under stirring at 800 rpm up to a final volume ratio of 5:1 (chitosan:TPP). Subsequently the resulting suspension was stirred for additional 30 min in order to get a stable particle formation. The particle suspension was centrifuged for 8 min at 1,677*g* to remove the excess of unreacted chitosan and TPP and the obtained sediment was suspended for further investigation in HEPES-buffered saline (HBS) of pH 6.8 (1 L contains: 5.2 g HEPES, 7.9 g NaCl, 1 g glucose, 373 mg KCl, 147 mg $CaCl_2$ dihydrate). β-Galactosidase loaded nanoparticles were prepared in the same way in addition of the 500 µL β-galactosidase (10 mg/mL in demineralized water) to the chitosan solution.

2.2.3. Nanoparticle characterization

Particle size, polydispersity index (PDI) and zeta potential of the nanoparticles were determined by photon correlation spectroscopy with NICOMP™ 380 ZLS PSS (Santa Barbara, CA, USA) with a laser wavelength of 650 nm and an E-field strength of 5 V/cm with an electrode spacing of 0.3 cm.

Particle yield was ascertained gravimetrically after centrifugation (8 min at 1,677*g*) and lyophilization (Christ Gamma 1–16 LSC Freeze dryer, Germany) of the nanoparticles.

Loading of β-galactosidase was determined upon centrifugation of the particle suspension by quantifying the residual amount of enzyme in the supernatant. Therefore the bicinchoninic acid assay was used. A solution of β-galactosidase in the same concentration as used for the nanoparticle preparation in water served as 100 % value. The encapsulation efficiency (EE) was calculated according to Eq. (1).

$$\text{EE (\%)} = \frac{\text{100\% value} - \text{protein amount in supernatant}}{\text{100\% value}} \times 100 \quad (1)$$

2.2.4. Nanoparticle degradation by isolated IAP

2.2.4.1. Dissolution of nanoparticles. Dissolution of the β-galactosidase loaded nanoparticles was examined under addition of isolated intestinal alkaline phosphatase (IAP). In brief, to 1 mL of the nanoparticle suspensions (0.074 % (m/m)) 1 Unit of IAP in aqueous solution was added. Suspensions were incubated at 37 °C for 4 h with 100 µL sampling at pre-determined time points. Dissolution of nanoparticles due to the cleavage of the ionic cross-linker TPP by IAP was evaluated while monitoring the changes in optical density of the suspensions over time by measuring the absorbance at 600 nm (TECAN Spark®, Tecan Group Ltd., Switzerland). In parallel particle size was measured before addition of IAP and after 4 h incubation at 37 °C. Particle samples omitting IAP were taken as controls.

2.2.4.2. Phosphate elimination. Phosphate release of the loaded nanoparticles due to the degradation of TPP induced by isolated IAP (1 U/mL) was assessed. Therefore, nanoparticles (0.074 % (m/m)) were subjected to 4 h incubation at 37 °C and 500 rpm agitation (ThermoMixer C, Eppendorf Vertrieb Deutschland GmbH, Germany). At defined time points 50 µL samplings were withdrawn and analyzed for their phosphate content employing the malachite green assay as described above under Section 2.2.1.1. Particles incubated without adding the enzyme served as controls.

2.2.5. Phosphate elimination on Caco-2 cells

Hydrolysis of the ionic cross-linker TPP and resulting phosphate elimination was further investigated in a cell based assay on Caco-2 cells [15]. In detail, cells were seeded on a 24-well cell culture plate with a seeding density of $5x10^4$ cells/well and were cultured for 9 days in minimum essential medium (MEM) supplemented with 10 % (v/v) fetal calf serum (FCS) and penicillin/streptomycin solution (100 U/mL, 100 µg/mL) at 37 °C in an atmosphere of 5 % CO_2 and 95 % relative humidity.

In order to find a tolerable concentration of nanoparticles, cell

viability was investigated in a resazurin assay [16,17] subsequent to incubation with various amounts of particles at 37 °C in an atmosphere of 5 % CO_2 and 95 % relative humidity. Following incubation, cells were washed with 500 µL HBS and thereafter 250 µL of a 5 % (m/v) resazurin solution in MEM without phenol red were added and for another period of 2 h incubated. Fluorescence of the supernatant was measured at 540 nm excitation wavelength and 590 nm emission wavelength (TECAN Spark®, Tecan Group Ltd., Switzerland). HBS was applied as positive control and a 1 % (m/m) solution of Triton X-100 in HBS as negative control.

Phosphate release by cell-associated IAP was explored while applying 750 µL of nanoparticles per well in a concentration of 0.007 % and 0.004 % (m/m). Cells incubated with nanoparticle samples spiked with 0.05 % (v/v) phosphatase inhibitor cocktail 2 and pre-incubated with 1 % inhibitor in HBS for 30 min served as controls. At predetermined time points aliquots of 50 µL were withdrawn and analyzed by malachite green assay.

2.2.6. Targeted release of β-galactosidase

In order to quantify the release of β-galactosidase from nanoparticles, suspensions (0.074 % (m/m)) were incubated with isolated IAP or on porcine intestinal mucosa at 37 °C.

2.2.6.1. β-Galactosidase release using isolated IAP. Nanoparticles were incubated using the same conditions and particle to IAP ratio as described under Section 2.2.4. The batch size was 5 mL and 500 µL samples were withdrawn at the set time points. After 2 min centrifugation at 6,708*g* supernatants were analyzed with BCA assay for their protein content.

2.2.6.2. β-Galactosidase release on porcine small intestinal mucosa. Porcine small intestine obtained from a local abattoir was cut into pieces and was mounted on Franz diffusion cells (orifice diameter 9 mm, Perme Gear, Inc, USA) with the luminal tissue side oriented to the top. Afterwards 1 mL of test solution was filled into the upper compartment followed by incubation at 37 °C. Samples pre-incubated with 1 % phosphatase inhibitor cocktail 2 for 1 h served as controls and the basic signal of the tissue was recorded by incubation with pure HBS. At predetermined time points, solutions were carefully removed, centrifuged for 2 min at 6,708*g* and the supernatants were analyzed by ONPG activity assay. The detected absorbance was correlated to the concentration of β-galactosidase by means of a standard curve prepared of decreasing concentrations of β-galactosidase.

2.2.7. Stability against digestion by trypsin

Enzymatic stability was investigated according to a method previously described [18]. Therefore a solution of trypsin was prepared in HBS with a activity of 9.35 IU/mL corresponding to physiological conditions [19]. This enzyme solution was tempered to 37 °C on a water bath (1083, GFL Gesellschaft für Labortechnik mbH, Germany) and was either added to an equally prewarmed solution of pure β-galactosidase (278.3 µg/mL) or nanoparticle suspension (0.074 % (m/m) in a volume ratio of 1:1. Subsequently, degradation studies were performed at 37 °C and 500 rpm (ThermoMixer C, Eppendorf Vertrieb Deutschland GmbH, Germany). Enzymatic activity of β-galactosidase was verified by ONPG assay at predefined time points. Samples lacking trypsin addition were considered as reference values in the calculation of the residual activity.

2.2.8. Statistical data analysis

All experiments and measurements were carried out at least in triplicate. Represented data are the means including standard deviation. The software Graph Pad Prism version 5.01 was used for the statistical data analysis. One way ANOVA and Bonferroni *t*-test were performed with $P < 0.05$ as the minimal level of significance.

3. Results and discussion

3.1. Nanoparticle preparation and characterization

Nanoparticles were prepared *via* ionic gelation method between positively charged chitosan and negatively charged TPP as cross-linking agent. Dropwise addition of TPP to the chitosan solution resulted in a turbid mixture, indicating the formation of nanoparticles. β-Galactosidase was selected as active ingredient because of two main reasons, first it might be expected that it underlies a pre-systemic enzymatic metabolism in the lumen of the small intestine [20,21] and therefore shielding by encapsulation in nanoparticles seems to be reasonable. Secondly the target location of β-galactosidase is at the brush border membrane of the enterocyte where it should be released according to the postulated concept. The decision to incorporate yeast β-galactosidase from *Kluyveromyces lactis* was made because it counts to the major enzymes used in dairy industry and in therapeutic products in order to treat lactose-intolerance problems [22]. Especially its mild optimal operating terms concerning pH range (6.6–7.0) and temperature (35–40 °C) are [23] ideally matching the conditions in the intestine.

Nanoparticles were obtained by centrifugation in a yield of 0.74 ± 0.11 mg/mL. As prepared nanoparticles appeared to be highly sensitive to centrifugation, parameters were selected to find a compromise between aggregation and satisfactory yield. Higher applied forces or subjection to longer times led to aggregation with recovered particles in the micron range. The incorporation of β-galactosidase did not affect the particle size, whereas the zeta potential decreased significantly ($P < 0.001$). Accordingly, a mean size of 784.4 ± 24.5 nm and a PDI of 0.207 ± 0.089 without β-galactosidase and 761.6 ± 35.3 nm with a PDI of 0.104 ± 0.045 with β-galactosidase in water was measured. A decrease in zeta potential from +27.6 ± 2.5 mV to +17.9 ± 2.1 mV upon loading of β-galactosidase was recorded, respectively. The zeta potential of the nanoparticles is predominantly defined by the primary amino groups of the chitosan. β-Galactosidase has an isoelectric point of 5.42 [23] and possesses a negative charge at neutral pH, consequently the decrease in overall net charge might be evoked by the partial deposition of the enzyme on the particle surface. Characteristics of the nanoparticles suspended in HBS are listed in Table 1. The high concentration of NaCl in HBS might lead

Table 1
Characterization of the β-galactosidase loaded nanoparticles regarding mean diameter, polydispersity index (PDI), encapsulation efficiency (EE) and incorporated amount of enzyme. Furthermore measured particle size as well as PDI of nanoparticles after 4 h incubation at 37 °C in absence and presence of 1 U/mL isolated intestinal alkaline phosphatase (IAP) are listed.

Particles	Mean diameter [nm]	PDI	EE [%]	β-Galactosidase [µg/mg particles]	β-Galactosidase [µg/mL particle suspension]
Resuspended in HBS pH 6.8	573.3 ± 34.2	0.352 ± 0.023	36.2 ± 1.8	376.0 ± 18.4	278.3 ± 13.6
Particle characteristics after 4 h incubation at 37 °C					
Without IAP		With 1 U/mL IAP			
Mean diameter [nm]	PDI	Mean diameter [nm]	PDI		
467.4 ± 20.7	0.346 ± 0.030	357.7 ± 20.8	0.189 ± 0.023		

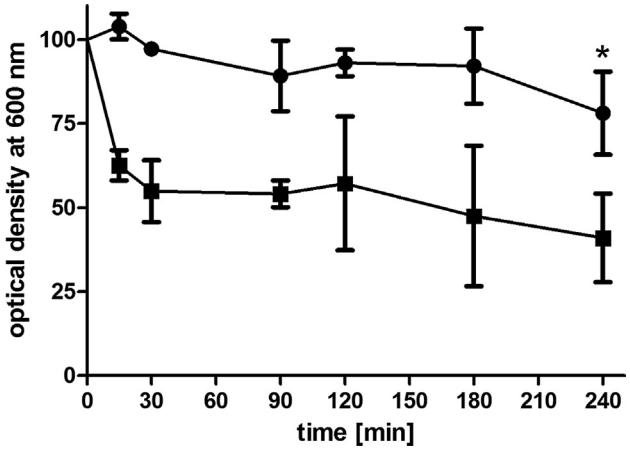

Fig. 1. Optical density of nanoparticle suspensions measured at 600 nm under incubation with 1 Unit/mL isolated IAP at 37 °C in HBS pH 6.8. Circles express data of β-galactosidase loaded particles and squares depict changes of the unloaded nanoparticles. Values are means of at least three experiments ± SD.

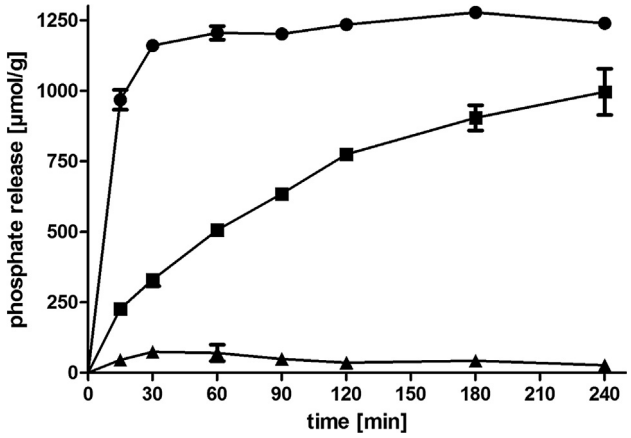

Fig. 2. Phosphate release over four hours incubation at 37 °C and 500 rpm in the absence (▲) and presence of 0.1 Units/mL (■) or 1 Unit/mL (●) isolated IAP. Nanoparticles were suspended in HBS pH 6.8. Indicated values represent data of at least three experiments ± SD.

to smaller particle size than obtained in water. Similar observations were made in previous studies where smaller particles and higher compacted complexes could be achieved with increasing content of monovalent salts in saline solvents [24,25].

3.2. Nanoparticle degradation by isolated IAP

3.2.1. Dissolution of nanoparticles

In theory there should be a direct correlation between phosphate release and nanoparticle stability. Hydrolysis of TPP ends up in a loosening of the particle network accompanied by its degradation and finally results in a decrease of optical density of the suspension. Therefore optical density of the particle suspensions was observed additionally to size measurements in order to further confirm nanoparticle degradation during incubation with isolated IAP, beside quantification of phosphate. The optical density of β-galactosidase loaded particles was reduced by 22 % after 4 h incubation. Unloaded nanoparticles were investigated for comparison and exhibited a decrease by 59 % (Fig. 1). Detected discrepancies in remaining turbidity might derive from the formation of partly insoluble chitosan/β-galactosidase complexes on account of the high affinity of negatively charged β-galactosidase to positively charged chitosan. Particle size (Table 1) was reduced by 37.6 ± 7.1 % after 4 h incubation in presence of IAP. Interestingly, the size of particles decreased as well in absence of IAP to a lesser extent by 18.5 ± 3.7 %. One possible explanation for this finding might be a decrease in intrinsic viscosity of chitosan being exposed to a higher solution temperature over time whilst promoting the formation of more compacted particles. Fan et al. [26] clarified this effect in more detail as a consequence of the decrease in the ratio of radius of gyration of chitosan and reduced hydrogen-bonded hydration water, resulting in an increase in chitosan flexibility along with a decrease in specific volume of the chitosan molecule. Supporting this argumentation PDI for the particle suspension missing IAP remained unchanged, suggesting a uniform decrease in size. On the contrary a 46.3 ± 6.5 % decline in PDI of nanoparticles incubated with IAP indicates a narrow size distribution as arising from particle degradation in connection with phosphatase mediated splitting of TPP.

3.2.2. Phosphate elimination

In order to liberate β-galactosidase in the desired target-oriented manner, the cross-linker TPP has to be hydrolyzed enzymatically by IAP. As the alkaline phosphatase has a broad substrate specifity TPP can be considered as a known substrate. Yoza et al. [27] demonstrated the cleavage of TPP by calf intestinal alkaline phosphatase at a physiologic pH of 7.2. Hence, enzymatic cleavage of the cross-linker TPP using isolated IAP was evaluated by detecting the released amount of free phosphate over time. Therefore IAP was added in two concentrations representing on the one hand a realistic concentration being present at the membrane of the enterocyte and on the other hand simulating a lower concentration of secreted IAP conceivably existent in mucus. Phosphate concentration in media increased in dependence on the amount of added IAP during a 4 h experiment, whereas the phosphate concentration in the control sample without IAP addition remained constant at a level around 5 µg of phosphate per mg of nanoparticles (Fig. 2). Reaction proceeded fast under addition of 1 U/mL IAP with a plateau reached after 30 min and a total amount of 118 ± 1 µg/mg particles of liberated phosphate. In case of a higher substrate to enzyme ratio under 0.1 Units IAP supplement, detected final phosphate level was lower with 95 ± 8 µg/mg and a plateau was not reached.

3.3. Phosphate elimination on Caco-2 cells

Phosphate release mediated by cell-associated IAP on the human adenocarcinoma cell line Caco-2 was evaluated in addition to experiments performed with isolated IAP. This cell line undergoes an enterocyte-like differentiation with the expression of a number of brush-border membrane associated enzymes, among them alkaline phosphatase [28]. In previous studies of our research group it was already proven that Caco-2 cells express enough IAP to cleave a variety of phosphate ester structures within nanoparticles [29–31], furthermore Prüfert et al. [30] visualized alkaline phosphatase on the cell surface employing immunocytochemistry. Pinto et al. [32] denoted the activity of alkaline phosphatase on Caco-2 cells to be approximately 50 % lower than in human intestine. With regard to the present protein amount, Jumarie and Malo [33] calculated activities in a range of 3–10 mU/mg protein depending on the culture duration between 5 and 21 days and an initial seeding density of 4×10^4 cells/cm^2. To inquire the ability of the cell-associated enzyme to cleave TPP cross-links inside of the particle network, phosphate release on a Caco-2 cell monolayer was monitored according to a similar protocol. First of all a resazurin assay was carried out to elucidate a proper test concentration of nanoparticles. Results summarized in Fig. 3 attest a concentration dependent effect with significant ($P < 0.001$) decreased cell viability caused by the higher concentration of nanoparticles and by the samples spiked with phosphatase inhibitor cocktail 2. Reduced viability of cells incubated with the inhibitor might be due to side effects triggered by sodium orthovanadate through processes such as inhibition of ATPases or enhanced oxidative stress [34]. Nevertheless, cell viability values were still above the generally acceptable threshold of 80 % to be

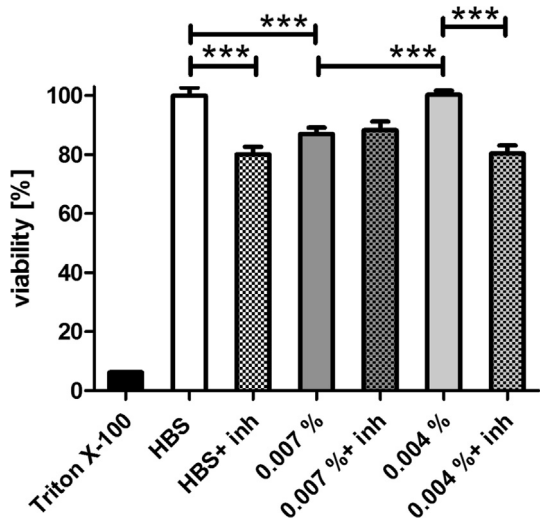

Fig. 3. Cell viability of Caco-2 cells after 4 h treatment with β-galactosidase loaded nanoparticles and controls in the absence and presence (+inh) of phosphatase inhibitor cocktail 2. Displayed values show the data of at least three experiments ± standard deviation.

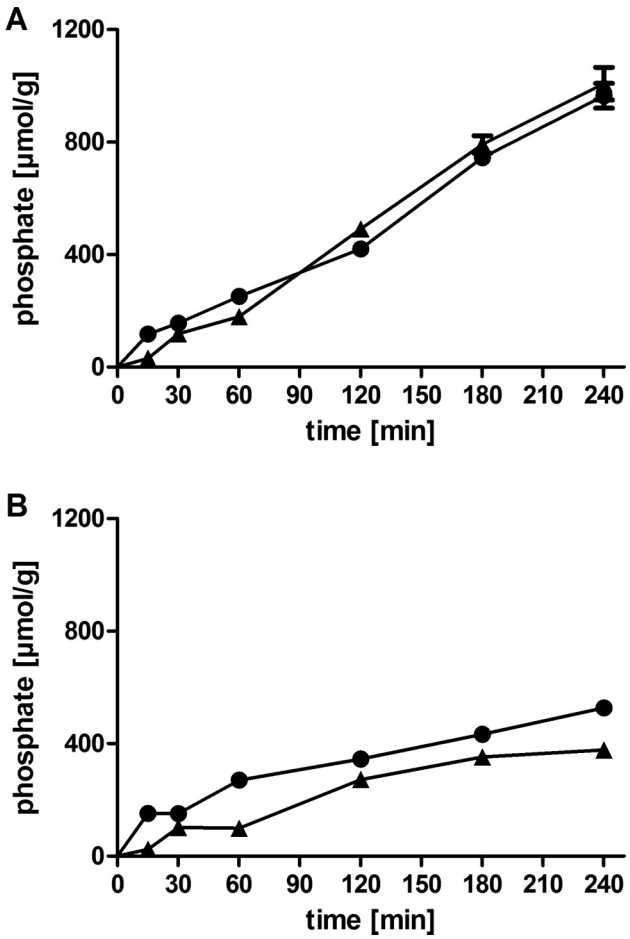

Fig. 4. Phosphate release from β-galactosidase loaded nanoparticles induced by cleavage of TPP by cell-associated IAP. Nanoparticles were applied in a concentration of 0.007 % (m/m) (●) and 0.004 % (m/m) (▲). Part A depicts the results without phosphatase inhibitor and Part B outlines the release from nanoparticles supplemented by 0.05 % (v/v) inhibitor. Indicated values represent the data of at least three experiments ± standard deviation.

considered as viable. Moreover cellular function was probably not impaired as neither detachment of cells could be observed, nor changes in morphology of the monolayer were visible and similar phosphate levels were evidenced for both concentrations (Fig. 4).

The calculated amount of phosphate after 4 h was similar to the results obtained under addition of 0.1 Unit/mL isolated IAP but the liberation was slower and continuous from the beginning without reaching saturation. This profile is strongly contrasting to the one obtained by isolated IAP and gives a hint at a lower amount of IAP present at the cell surface, as compared to the concentration of free enzyme used, along with an excess of available substrate. As shown in Fig. 4B phosphatase activity of the control cells was not completely suppressed under treatment with the inhibitor. While having a nearly 2-fold (0.007 %) and 2.5-fold (0.004 %) lower signal than the probes, results are in line with the observations of Le-Vinh et al. [35]. The outcome of these phosphate liberation studies clearly demonstrate the ability of IAP, whether free or membrane-bound, to hydrolyze TPP and consequently degrade the nanoparticles.

3.4. Targeted release of β-galactosidase

3.4.1. β-Galactosidase release using isolated IAP

IAP triggered release of incorporated β-galactosidase from nanoparticles was confirmed by a 2.5-fold elevated enzyme content in the release medium compared to the control omitting phosphatase addition. A plateau phase reached after 60 min marked the completion of β-galactosidase release to a total amount of 57.5 ± 0.5 % with regard to the initial loading (Fig. 5). The extent of β-galactosidase in the control indicated a leaking out during the experiment probably evoked by diffusion of loosely adherent enzyme from the particle surface.

3.4.2. β-Galactosidase release on porcine small intestinal mucosa

Results from Caco-2 cells already pointed out the capability of a living system to cleave TPP and formed a base for the assumption of equal findings in a tissue based experiment. Hence, target dependent liberation of β-galactosidase was further examined on porcine intestinal mucosa. After 3 h 94 % of the initial amount of incorporated enzyme was released (Fig. 6, striped bar). Under the assumption that the activity of IAP bound on mucosa exceeds the amount applied in the phosphate elimination study, superior liberation of the payload can be justified. A delayed enzyme release was assumed, as nanoparticles have to move first across the entire mucus layer in order to reach the brush border membrane. This presumption could be confirmed by our studies showing a retarded release after one hour compared to the experiment with isolated IAP (Fig. 5). Pre-incubation with the phosphatase

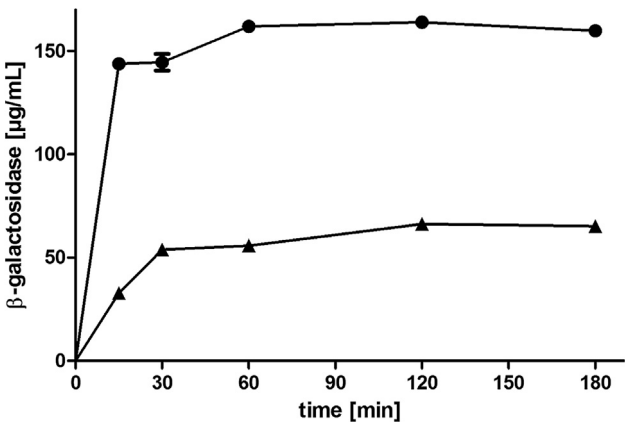

Fig. 5. Release of β-galactosidase from nanoparticles in presence (●) and absence (▲) of 1 U/mL isolated IAP. Experiment was performed in HBS pH 6.8 at 37 °C and 500 rpm. Specified values represent the data of at least three experiments ± standard deviation.

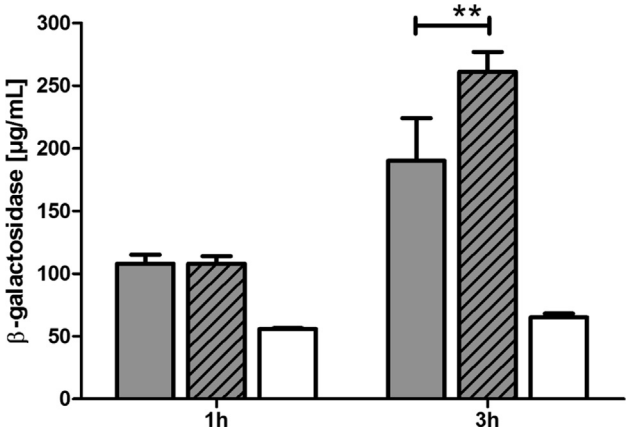

Fig. 6. Release of β-galactosidase from nanoparticles during a three hours incubation on porcine intestinal mucosa at 37 °C in HBS pH 6.8. Blank grey bars depict the detected amount of enzyme on tissue samples pre-incubated with 1 % (v/v) phosphatase inhibitor whereas striped bars portray the values of samples omitting inhibitor treatment. White bars display the amount of β-galactosidase leaking calculated by BCA assay. Values represent the data of at least three experiments ± standard deviation.

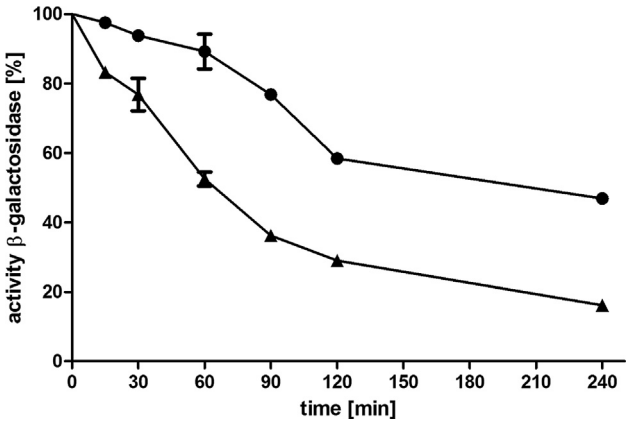

Fig. 7. Remaining enzymatic activity of β-galactosidase under 4 h incubation with 4.675 IU/mL trypsin in HBS pH 6.8 at 37 °C. Circles depict the results of the nanoparticles and triangles represent those of pure β-galactosidase. Values are the means of at least three experiments ± standard deviation.

inhibitor cocktail 2 (Fig. 6, blank grey bars) could diminish the activity of IAP to an even less extent as on Caco-2 cells, probably due to the higher concentration of phosphatase on the monolayer. Consequently, the outcome of this β-galactosidase liberation study on the mucosa supports the hypothesis that a targeted induced cleavage and release can occur in connection with a mucus permeation of the particles. Even though the postulated principle seems to work, the entire release of β-galactosidase should be assessed in a more critical manner. In general particles with a size approaching a cut-off size of 500 nm are supposed to be sterically trapped in mucus, irrespective of their surface chemistry due to the average mucus pore size of 200 nm [36,37]. Nevertheless diffusion of particles as large as 500 nm or even larger inside of porcine jejunal mucus and human mucus gels was already reported in previous studies [38–41]. Premature cleavage by secreted IAP and release of the payload in mucus might also occur and contribute together with the higher activity of IAP on tissue to the high release. As long as the β-galactosidase reaches the mucus layer still incorporated in particles it should be protected against luminal enzymatic degradation. Therefore a release in mucus might not have a pronounced adverse effect on the delivery system's performance in the intestine as trypsin concentration in mucus is negligible.

3.5. Stability against digestion by trypsin

For the purpose of successful delivery of therapeutic enzymes one major point that has to be addressed is the protection against luminal degradation by proteases until the mucus layer which provides shielding against enzymatic attack is reached. Proteolytic stability of β-galactosidase was investigated while using trypsin as one of the most relevant pancreatic serine endopeptidases being present in the lumen of the small intestine. Trypsin cleaves internal peptide bonds in most peptides and proteins preferably near by arginine, lysine and aromatic amino residues [42,43]. β-Galactosidase of *E. coli* can be cleaved by trypsin [20] into 65 fragments over the course of complete hydrolysis [44]. Furthermore β-galactosidase in strains of *Propionibacterium freudenreichii* was inactivated by tryptic degradation [21]. Owing to extended sequence homologies with several published prokaryotic β-galactosidase sequences, among them *E. coli* [45], it can be presumed that β-galactosidase from *Kluyveromyces lactis* is a target of trypsin as well. Enzymatic activity of β-galactosidase encapsulated in nanoparticles was preserved to a 3-fold higher extent as in a control containing the same amount of free β-galactosidase (Fig. 7). According to this result it can be expected that the nanoparticles can function as a shelter while suppressing luminal proteolysis.

4. Conclusion

Within the scope of this study the suitability of chitosan/TPP nanoparticles in order to achieve a targeted release system was proven. Using ionic gelation, the model drug β-galactosidase could be successfully encapsulated. The results obtained from different degradation tests with isolated as well as cell-associated IAP showed a good correlation. Additionally a release study of β-galactosidase in a tissue based experiment gave a hint that the system might be able to pass the mucus barrier and reach the absorption epithelia as IAP mediated liberation was confirmed. Consequently this system can be presented as a promising carrier capable to transport its therapeutic ingredient to the intestinal brush border membrane and finally degrade in a targeted controlled manner in contact with the IAP. Further studies on other mucosal tissues expressing alkaline phosphatases might be interesting to evaluate the consistency of the release concept.

References

[1] E. Moroz, S. Matoori, J.C. Leroux, Oral delivery of macromolecular drugs: Where we are after almost 100years of attempts, Adv. Drug Deliv. Rev. 101 (2016) 108–121.
[2] B.F. Choonara, Y.E. Choonara, P. Kumar, D. Bijukumar, L.C. du Toit, V. Pillay, A review of advanced oral drug delivery technologies facilitating the protection and absorption of protein and peptide molecules, Biotechnol. Adv. 32 (2014) 1269–1282.
[3] R. Bodmeier, H.G. Chen, O. Paeratakul, A novel approach to the oral delivery of micro- or nanoparticles, Pharm. Res. 6 (1989) 413–417.
[4] P. Calvo, C. Remunan-Lopez, J.L. Vila-Jato, M.J. Alonso, Chitosan and chitosan/ethylene oxide-propylene oxide block copolymer nanoparticles as novel carriers for proteins and vaccines, Pharm. Res. 14 (1997) 1431–1436.
[5] A. Rampino, M. Borgogna, P. Blasi, B. Bellich, A. Cesaro, Chitosan nanoparticles: preparation, size evolution and stability, Int. J. Pharm. 455 (2013) 219–228.
[6] Z. He, J.L. Santos, H. Tian, H. Huang, Y. Hu, L. Liu, K.W. Leong, Y. Chen, H.Q. Mao, Scalable fabrication of size-controlled chitosan nanoparticles for oral delivery of insulin, Biomaterials 130 (2017) 28–41.
[7] J.L. Millan, Alkaline phosphatases: structure, substrate specificity and functional relatedness to other members of a large superfamily of enzymes, Purinergic Signal 2 (2006) 335–341.
[8] K.M. Holtz, B. Stec, E.R. Kantrowitz, A model of the transition state in the alkaline phosphatase reaction, J. Biol. Chem. 274 (1999) 8351–8354.
[9] Y. Shun, I.D. McKelvie, B.T. Hart, Determination of alkaline phosphatase-hydrolyzable phosphorus in natural water systems by enzymatic flow injection, Limnol. Oceanogr. 39 (1994) 1993–2000.
[10] B. Misselwitz, D. Pohl, H. Fruhauf, M. Fried, S.R. Vavricka, M. Fox, Lactose malabsorption and intolerance: pathogenesis, diagnosis and treatment, United European Gastroenterol. J. 1 (2013) 151–159.
[11] Y. Vandenplas, Lactose intolerance, Asia Pac. J. Clin. Nutr. 24 (Suppl 1) (2015) S9–13.
[12] A.A. Baykov, O.A. Evtushenko, S.M. Avaeva, A malachite green procedure for orthophosphate determination and its use in alkaline phosphatase-based enzyme

immunoassay, Anal. Biochem. 171 (1988) 266–270.
[13] N.G. Asp, A. Dahlqvist, O. Koldovsky, Human small-intestinal beta-galactosidases. Separation and characterization of one lactase and one hetero beta-galactosidase, Biochem. J. 114 (1969) 351–359.
[14] A. Bernkop-Schnürch, A. Weithaler, K. Albrecht, A. Greimel, Thiomers: preparation and in vitro evaluation of a mucoadhesive nanoparticulate drug delivery system, Int. J. Pharm. 317 (2006) 76–81.
[15] G. Perera, M. Zipser, S. Bonengel, W. Salvenmoser, A. Bernkop-Schnürch, Development of phosphorylated nanoparticles as zeta potential inverting systems, Eur. J. Pharm. Biopharm.: Off. J. Arbeitsgemeinschaft fur Pharmazeutische Verfahrenstechnik e.V 97 (2015) 250–256.
[16] J. O'Brien, I. Wilson, T. Orton, F. Pognan, Investigation of the Alamar Blue (resazurin) fluorescent dye for the assessment of mammalian cell cytotoxicity, Eur. J. Biochem. 267 (2000) 5421–5426.
[17] P. Jennings, C. Koppelstaetter, S. Aydin, T. Abberger, A.M. Wolf, G. Mayer, W. Pfaller, Cyclosporine A induces senescence in renal tubular epithelial cells, Am. J. Physiol. Renal. Physiol. 293 (2007) F831–838.
[18] F. Hintzen, G. Perera, S. Hauptstein, C. Müller, F. Laffleur, A. Bernkop-Schnürch, In vivo evaluation of an oral self-microemulsifying drug delivery system (SMEDDS) for leuprorelin, Int. J. Pharm. 472 (2014) 20–26.
[19] A. Bernkop-Schnürch, The use of inhibitory agents to overcome the enzymatic barrier to perorally administered therapeutic peptides and proteins, J. Control. Release 52 (1998) 1–16.
[20] A.V. Fowler, I. Zabin, The amino acid sequence of beta-galactosidase of Escherichia coli, Proc. Natl. Acad. Sci. USA 74 (1977) 1507–1510.
[21] G. Zárate, A.P. Chaia, S. González, G. Oliver, Viability and β-galactosidase activity of dairy propionibacteria subjected to digestion by artificial gastric and intestinal fluids, J. Food Protect. 63 (2000) 1214–1221.
[22] S.R. Tello-Solis, J. Jimenez-Guzman, C. Sarabia-Leos, L. Gomez-Ruiz, A.E. Cruz-Guerrero, G.M. Rodriguez-Serrano, M. Garcia-Garibay, Determination of the secondary structure of Kluyveromyces lactis beta-galactosidase by circular dichroism and its structure-activity relationship as a function of the pH, J. Agric. Food Chem. 53 (2005) 10200–10204.
[23] Q.Z.K. Zhou, X.D. Chen, Effects of temperature and pH on the catalytic activity of the immobilized β-galactosidase from Kluyveromyces lactis, Biochem. Eng. J. 9 (2001) 33–40.
[24] Y. Huang, Y. Lapitsky, On the kinetics of chitosan/tripolyphosphate micro- and nanogel aggregation and their effects on particle polydispersity, J. Colloid Interface Sci. 486 (2017) 27–37.
[25] H. Jonassen, A.L. Kjoniksen, M. Hiorth, Stability of chitosan nanoparticles cross-linked with tripolyphosphate, Biomacromolecules 13 (2012) 3747–3756.
[26] W. Fan, W. Yan, Z. Xu, H. Ni, Formation mechanism of monodisperse, low molecular weight chitosan nanoparticles by ionic gelation technique, Colloids Surf. B, Biointerfaces 90 (2012) 21–27.
[27] N. Yoza, S. Onoue, Y. Kuwahara, Catalytic ability of alkaline phosphatase to promote P-O-P bond hydrolyses of inorganic diphosphate and triphosphate, Chem. Lett. 26 (1997) 491–492.
[28] H. Matsumoto, R.H. Erickson, J.R. Gum, M. Yoshioka, E. Gum, Y.S. Kim, Biosynthesis of alkaline phosphatase during differentiation of the human colon cancer cell line Caco-2, Gastroenterology 98 (1990) 1199–1207.
[29] S. Bonengel, F. Prüfert, G. Perera, J. Schauer, A. Bernkop-Schnürch, Polyethylene imine-6-phosphogluconic acid nanoparticles–a novel zeta potential changing system, Int. J Pharm. 483 (2015) 19–25.
[30] F. Prüfert, S. Bonengel, S. Köllner, J. Griesser, M.D. Wilcox, P.I. Chater, J.P. Pearson, A. Bernkop-Schnürch, zeta potential changing nanoparticles as cystic fibrosis transmembrane conductance regulator gene delivery system: an in vitro evaluation, Nanomedicine (London, England) 12 (2017) 2713–2724.
[31] I. Nazir, C. Leichner, B. Le-Vinh, A. Bernkop-Schnürch, Surface phosphorylation of nanoparticles by hexokinase: a powerful tool for cellular uptake improvement, J. Colloid Interface Sci. 516 (2018) 384–391.
[32] M. Pinto, S. Robine, M.D. Appay, Enterocyte-like differentiation and polarization of the human colon carcinoma cell line CACO-2 in culture, 1983.
[33] C. Jumarie, C. Malo, Alkaline phosphatase and peptidase activities in Caco-2 cells: differential response to triiodothyronine, in vitro cellular & developmental biology, Animal 30a (1994) 753–760.
[34] Z.M. Delwar, D. Avramidis, E. Follin, Y. Hua, Å. Siden, M. Cruz, K.M. Paulsson, J.S. Yakisich, Cytotoxic effect of menadione and sodium orthovanadate in combination on human glioma cells, Investig. New Drugs 30 (2012) 1302–1310.
[35] B. Le-Vinh, N.N. Le, I. Nazir, B. Matuszczak, A. Bernkop-Schnürch, Chitosan based micelle with zeta potential changing property for effective mucosal drug delivery, Int. J. Biol. Macromol. 133 (2019) 647–655.
[36] A.N. Round, N.M. Rigby, A. Garcia de la Torre, A. Macierzanka, E.N.C. Mills, A.R. Mackie, Lamellar structures of MUC2-rich mucin: a potential role in governing the barrier and lubricating functions of intestinal mucus, Biomacromolecules 13 (2012) 3253–3261.
[37] X. Murgia, B. Loretz, O. Hartwig, M. Hittinger, C.-M. Lehr, The role of mucus on drug transport and its potential to affect therapeutic outcomes, Adv. Drug Deliv. Rev. 124 (2018) 82–97.
[38] A. Macierzanka, N.M. Rigby, A.P. Corfield, N. Wellner, F. Böttger, E.N.C. Mills, A.R. Mackie, Adsorption of bile salts to particles allows penetration of intestinal mucus, Soft Matter 7 (2011) 8077–8084.
[39] S.K. Lai, D.E. Hanlon, S. Harrold, S.T. Man, Y.-Y. Wang, R. Cone, J. Hanes, Rapid transport of large polymeric nanoparticles in fresh undiluted human mucus, Proc. Natl. Acad. Sci. 104 (2007) 1482.
[40] R.A. Cone, Barrier properties of mucus, Adv. Drug Deliv. Rev. 61 (2009) 75–85.
[41] G. Aljayyoussi, M. Abdulkarim, P. Griffiths, M. Gumbleton, Pharmaceutical nanoparticles and the mucin biopolymer barrier, Bioimpacts 2 (2012) 173–174.
[42] P. Langguth, V. Bohner, J. Heizmann, H.P. Merkle, S. Wolffram, G.L. Amidon, S. Yamashita, The challenge of proteolytic enzymes in intestinal peptide delivery, J. Control. Release 46 (1997) 39–57.
[43] G. Fuhrmann, J.-C. Leroux, Improving the stability and activity of oral therapeutic enzymes—recent advances and perspectives, Pharm. Res. 31 (2014) 1099–1105.
[44] Z.-H. Huang, T. Shen, J. Wu, D.A. Gage, J.T. Watson, Protein sequencing by matrix-assisted laser desorption ionization-postsource decay–mass spectrometry analysis of the N-Tris(2,4,6-trimethoxyphenyl)phosphine-acetylated tryptic digests, Anal. Biochem. 268 (1999) 305–317.
[45] O. Poch, H. L'Hôte, V. Dallery, F. Debeaux, R. Fleer, R. Sodoyer, Sequence of the Kluyveromyces lactis β-galactosidase: comparison with prokaryotic enzymes and secondary structure analysis, Gene 118 (1992) 55–63.